Meeting of ARES collaboration
GSI, 13 November 2014

INFN activities inside the ARES framework

L. Celona, G. Ciavola, S. Gammino, D. Mascali, G. Torrisi,
O. Leonardi, G. Castro, C. Caliri, C. Altana
Istituto Nazionale di Fisica Nucleare – Laboratori Nazionali del Sud

A. Galatà
Istituto Nazionale di Fisica Nucleare – Laboratori Nazionali di Legnaro

Deviation of ECRIS physics from classical models: experimental evidences

Non linear response of beam current (i.e. plasma density and lifetime) w.r.t. pumping frequency tuning

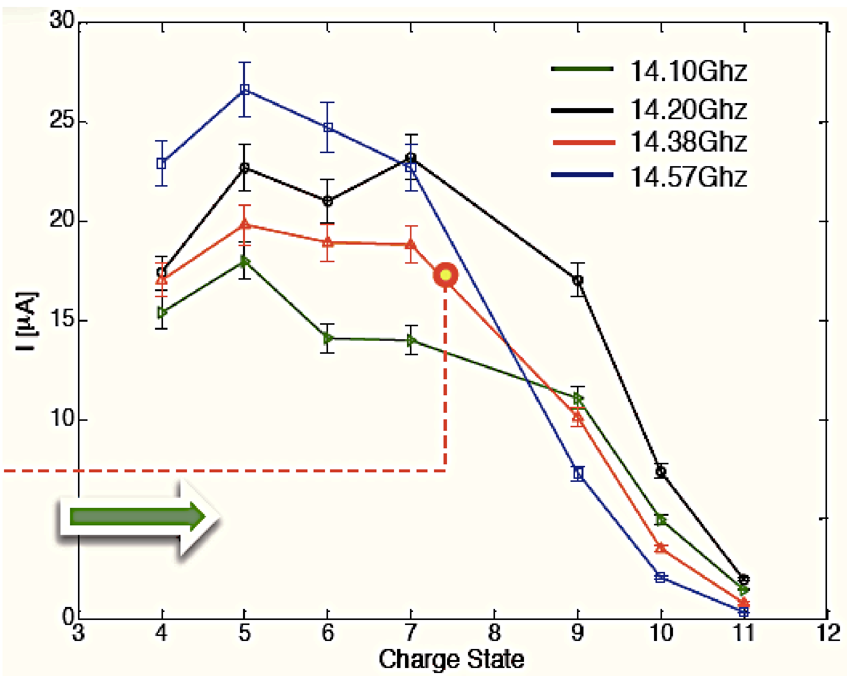

Non linear response of beam current (i.e. plasma density and lifetime) w.r.t. external magnetic field

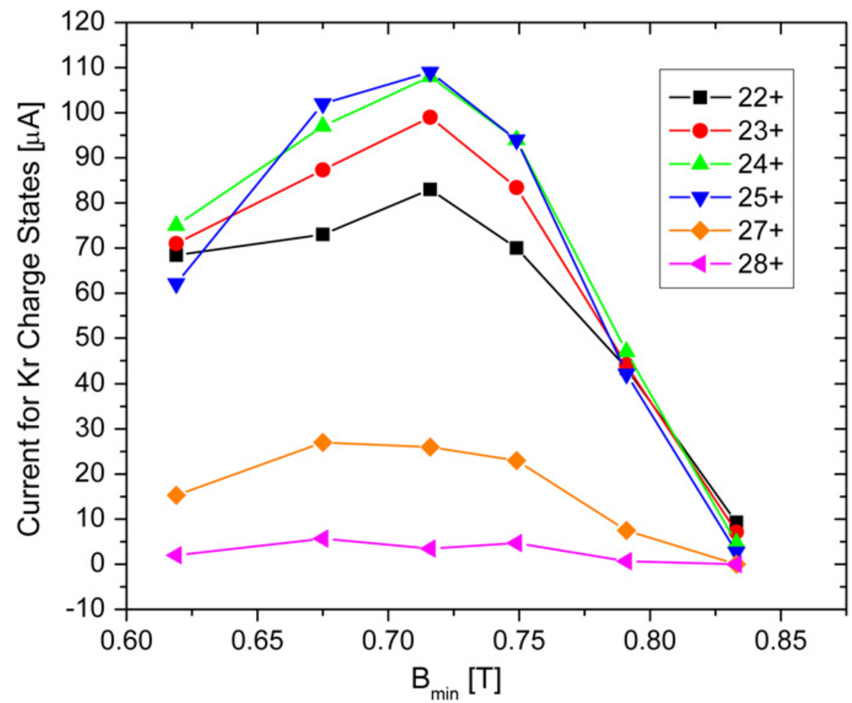

- Variations of few % in the pumping wave frequency or applied magnetostatic field change remarkably the source performances.
- This behaviour is not predicted by the classical model, which requires large scale variations of the frequency (several GHz, not few MHz) or the magnetic field (several kGs)

The pumping wave frequency as a "knob" for modifying the "warm" plasma component

The magnetostatic field at the ECR is a very sensitive "knob" for modifying the "hot" plasma component: to be handled with care!!

Changes in the cavity modal structure modify the heating rapidity

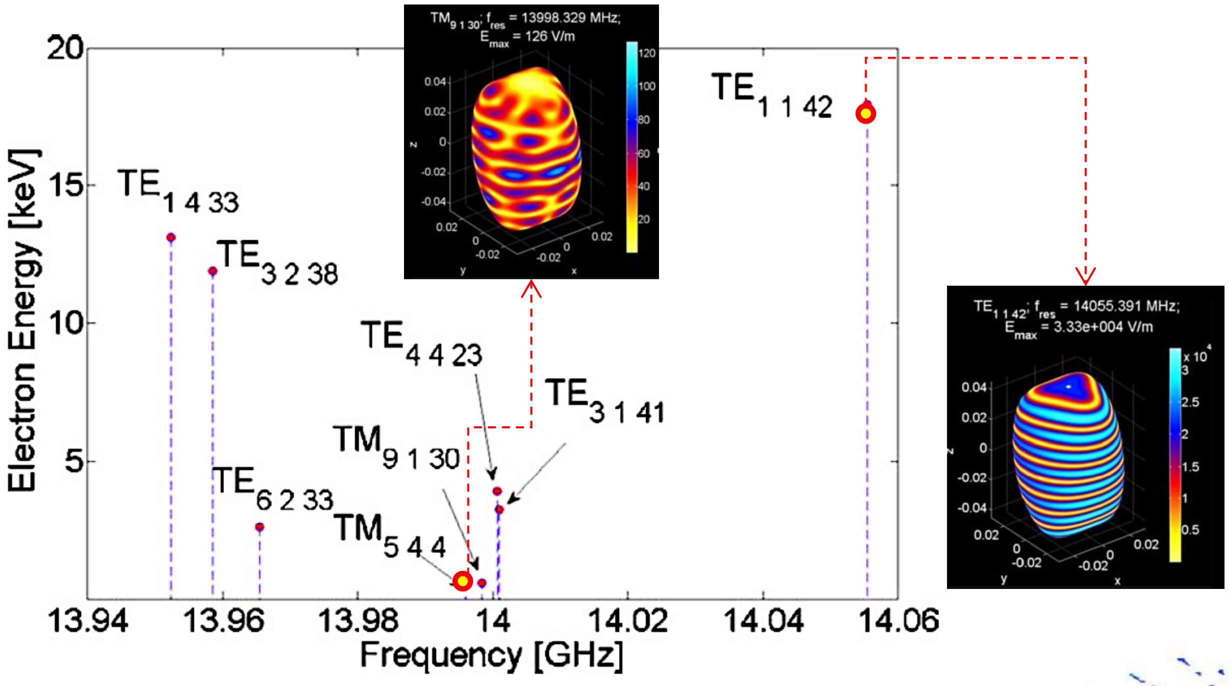

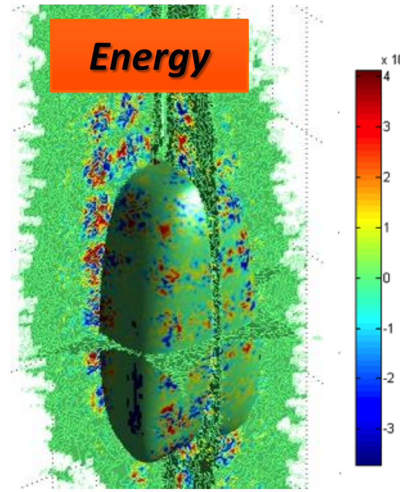

Localization of electrons energy absorption regions

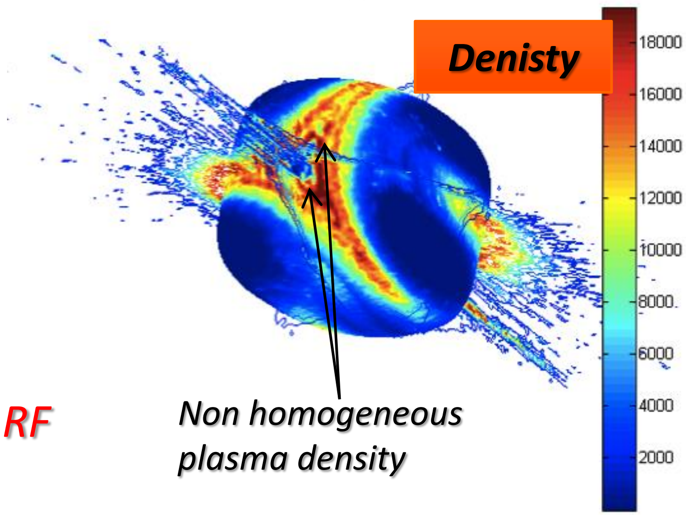

- *The wave frequency, determining resonant modes structures into the plasma chamber, changes the average energy gain rate which takes to the warm plasma formation*

- *The localization of energy deposition, along with the RF role in electron confinement, makes the density distribution irregular*

At the ECR, heating means also enhanced confinement, therefore the modal structure influences also the plasma shape

Injection side

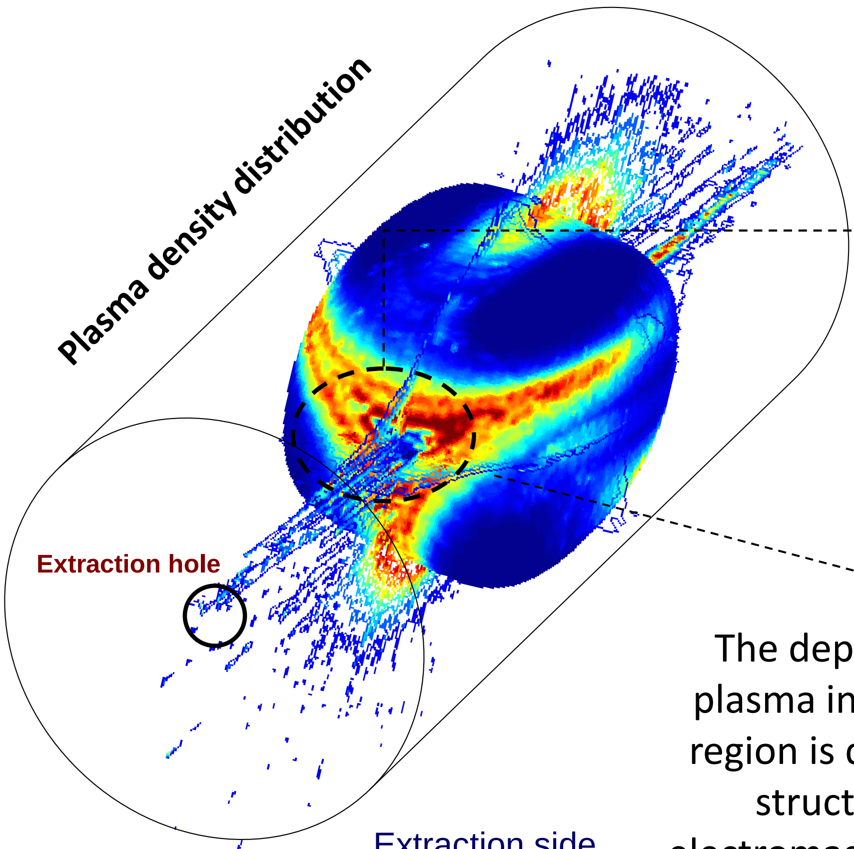

Extraction side

The density distribution explains why for some frequencies the beams appear hollow

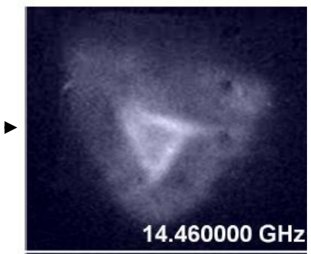

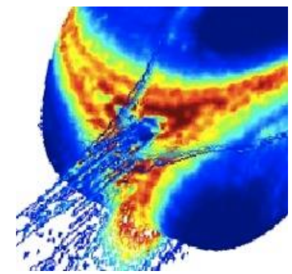

The depletion of plasma in near axis region is due to the structure of electromagnetic field.

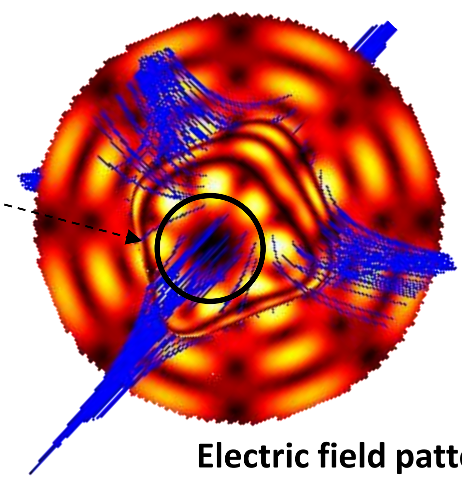

Electric field pattern

Near axis density depletion takes place because of low EM field. **Most of the resonant modes at f>10GHz exhibit holes in near axis zone**

- ***The model qualitatively explains the relationship between frequency, density and temperature.***

- ***But it includes only vacuum cavity modes in calculations, not the feedback of the plasma on the wave….***

Numerical Approaches for plasma modeling in Ion Sources

Already developed and under way

- *Numerical Code evaluating single particle kinetics*
- *RF coupling (full wave calculations) → FEM solvers*
- *Self-consistent strategies*

Perspectives

- *Coupling to Extraction&Transport*

Non-uniform dielectric tensor

In the cold approximation, the magnetostatic field is always represented with a vector along the z-axis. NOT APPLIABLE FOR ECRIS!!!

Non-symmetric 3D magnetostatic field equations

$$\begin{cases} B_x = B_1 xz + 2S_{ex} xy \\ B_y = -B_1 yz + S_{ex}(x^2 - y^2) \\ B_z = B_0 + B_1 z^2 \end{cases}$$

Assuming a non uniform magnetostatic field the ***dielectric tensor*** *is:*

$$\overline{\overline{\epsilon}} = \epsilon_0 \overline{\overline{\epsilon}}_r = \epsilon_0 \left(\overline{\overline{\mathrm{I}}} + \frac{\mathrm{i}\overline{\overline{\sigma}}}{\omega \epsilon_0} \right) = \epsilon_0 \left(\overline{\overline{\mathrm{I}}} + \frac{\mathrm{i}\omega_p^2 \overline{\overline{\mathrm{T}}}^{-1}}{\omega} \right) =$$

$$= \epsilon_0 \begin{bmatrix} 1 + \frac{\mathrm{i}\omega_p^2}{\omega} \frac{(-\mathrm{i}\omega + \omega_{\text{eff}})^2 + B_{0x}^2 (\frac{q}{m})^2}{\Delta} & \frac{\mathrm{i}\omega_p^2}{\omega} \frac{B_{0z} \frac{q}{m} (-\mathrm{i}\omega + \omega_{\text{eff}}) + B_{0x} B_{0y} (\frac{q}{m})^2}{\Delta} & \frac{\mathrm{i}\omega_p^2}{\omega} \frac{-B_{0y} \frac{q}{m} (-\mathrm{i}\omega + \omega_{\text{eff}}) + B_{0x} B_{0z} (\frac{q}{m})^2}{\Delta} \\ \frac{\mathrm{i}\omega_p^2}{\omega} \frac{-B_{0z} \frac{q}{m} (-\mathrm{i}\omega + \omega_{\text{eff}}) + B_{0x} B_{0y} (\frac{q}{m})^2}{\Delta} & 1 + \frac{\mathrm{i}\omega_p^2}{\omega} \frac{(-\mathrm{i}\omega + \omega_{\text{eff}})^2 + B_{0y}^2 (\frac{q}{m})^2}{\Delta} & \frac{\mathrm{i}\omega_p^2}{\omega} \frac{B_{0x} \frac{q}{m} (-\mathrm{i}\omega + \omega_{\text{eff}}) + B_{0y} B_{0z} (\frac{q}{m})^2}{\Delta} \\ \frac{\mathrm{i}\omega_p^2}{\omega} \frac{B_{0y} \frac{q}{m} (-\mathrm{i}\omega + \omega_{\text{eff}}) + B_{0x} B_{0z} (\frac{q}{m})^2}{\Delta} & \frac{\mathrm{i}\omega_p^2}{\omega} \frac{-B_{0x} \frac{q}{m} (-\mathrm{i}\omega + \omega_{\text{eff}}) + B_{0z} B_{0y} (\frac{q}{m})^2}{\Delta} & 1 + \frac{\mathrm{i}\omega_p^2}{\omega} \frac{(-\mathrm{i}\omega + \omega_{\text{eff}})^2 + B_{0z}^2 (\frac{q}{m})^2}{\Delta} \end{bmatrix}$$

$$\overline{\overline{\sigma}} = \epsilon_0 \omega_p^2 \overline{\overline{\mathrm{T}}}^{-1}$$

Off-diagonal Elements due to 3D Magnetic field

Full-wave computations

Journal of Electromagnetic Waves and Applications, 2014
Vol. 28, No. 9, 1085–1099, http://dx.doi.org/10.1080/09205071.2014.905245

Taylor & Francis
Taylor & Francis Group

Full-wave FEM simulations of electromagnetic waves in strongly magnetized non-homogeneous plasma

G. Torrisi[a,b*], D. Mascali[a], G. Sorbello[a,c], L. Neri[a], L. Celona[a], G. Castro[a], T. Isernia[b] and S. Gammino[a]

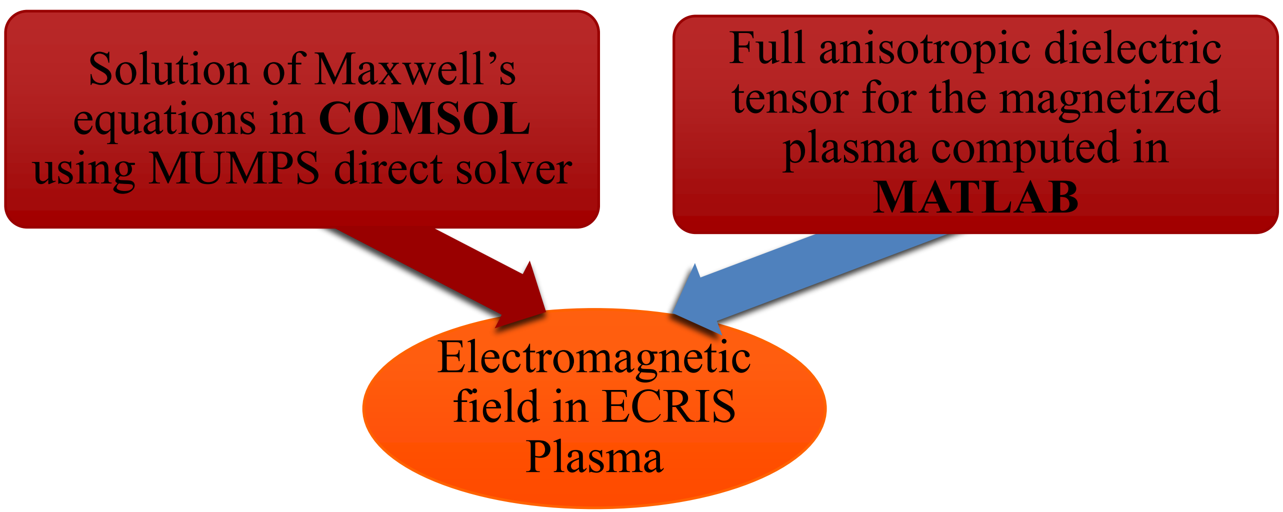

Full-wave computation: *8 GHz microwaves into the plasma filled chamber*

In-vacuum cavity field

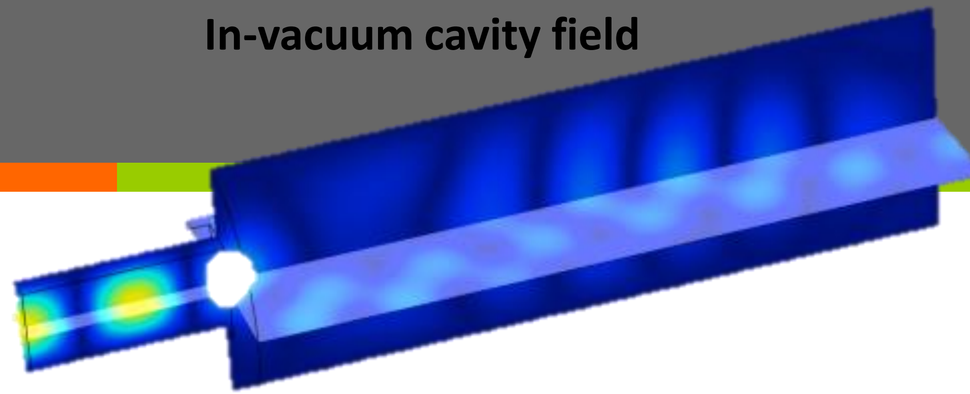

Non-uniform mesh accounting for dielectric tensor elements discontinuity at ECR

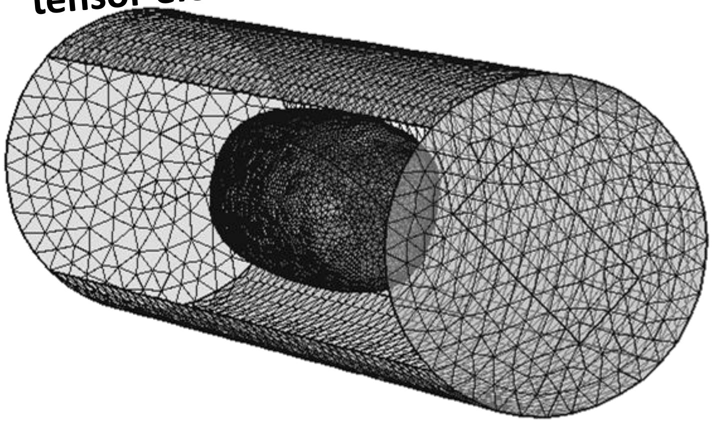

Electromagnetic field distribution inside the plasma filled cavity (cutoff density into the plasmoid)

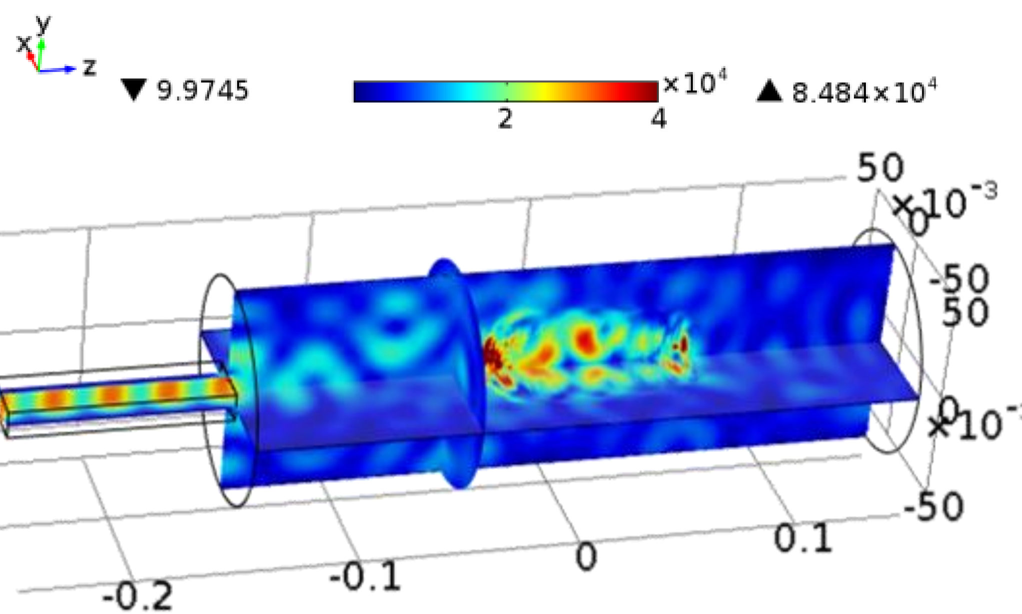

Self-consistency implementation

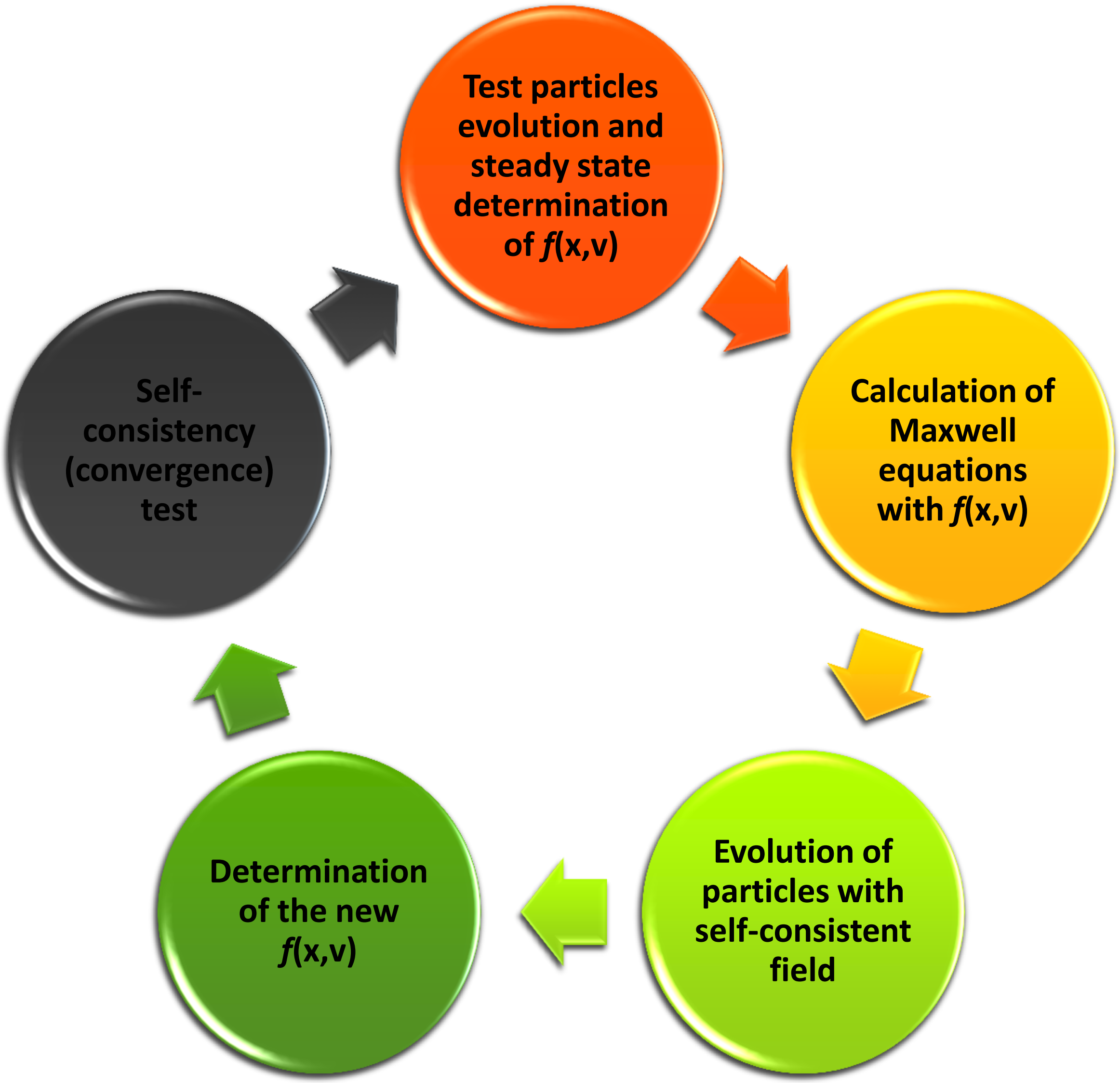

Simulations and modelling: Further Steps towards self-consistency

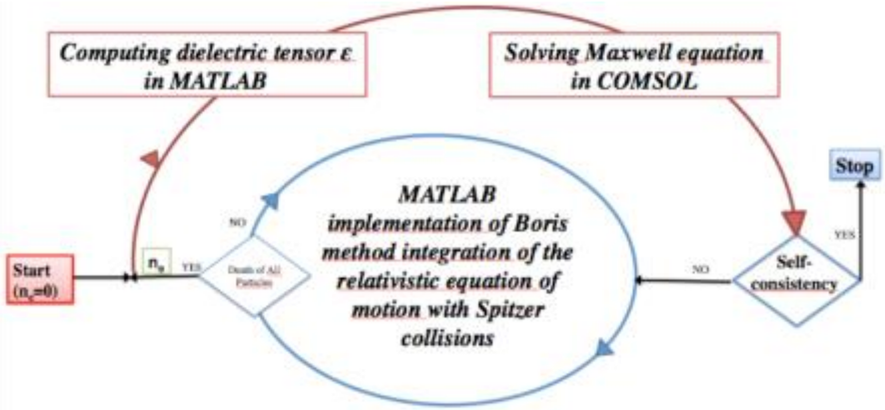

Solution of Maxwell-equations including the plasma inside the resonator: cold dielectric tensor used, accounting for R,L,O,X modes.

RF power deposition on the plasmoid surface

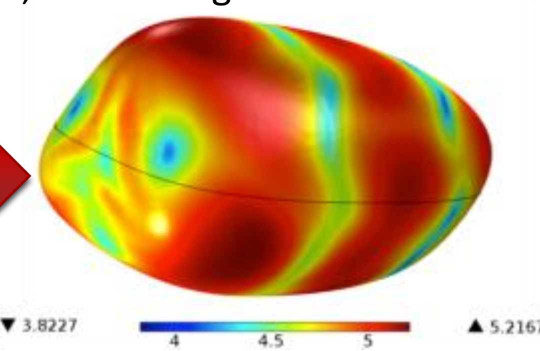

Plasma density structure in different energy domains

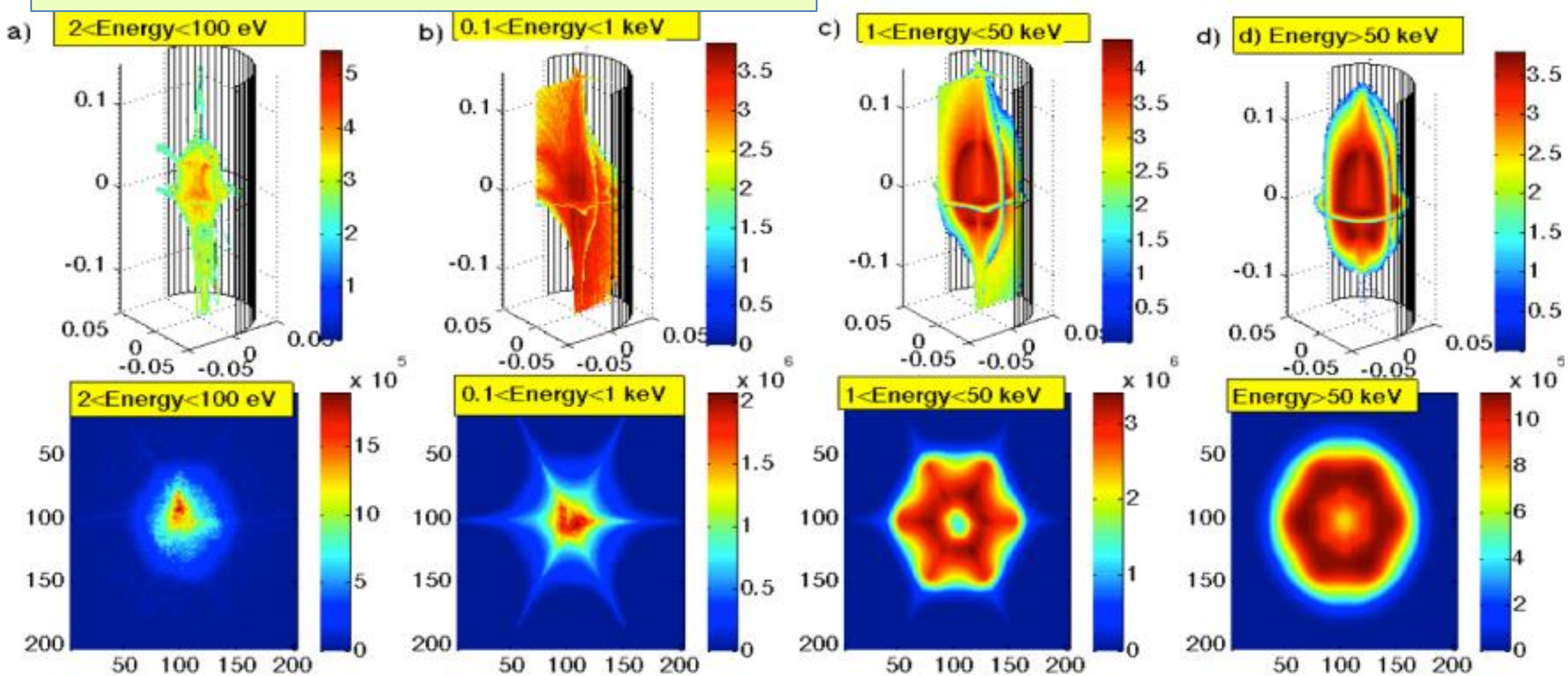

Codes and modeling

3D structure of the electron density: 1000 W RF, 1 eV init. Temp., 10^4 particles

KEY RESULT

plugging of plasma into the resonance surface and separation of the plasmoid from the plasma halo

The high density plasma is stably contained into the resonance surface

plasmoid generation

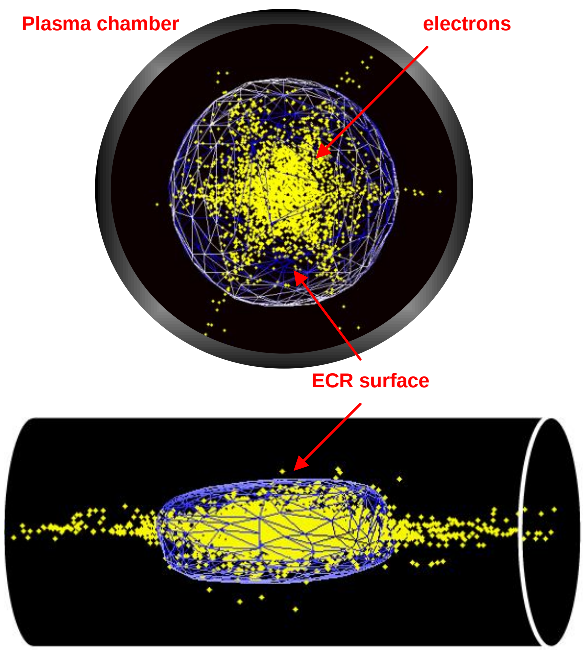

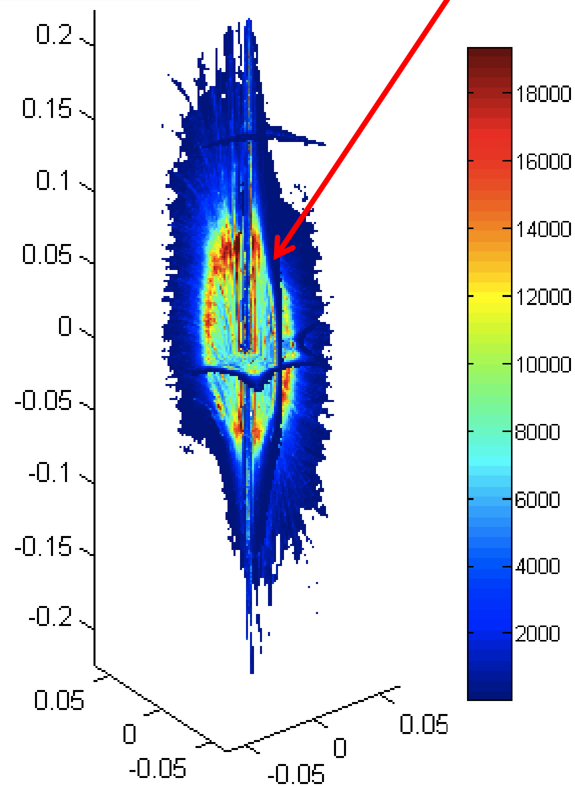

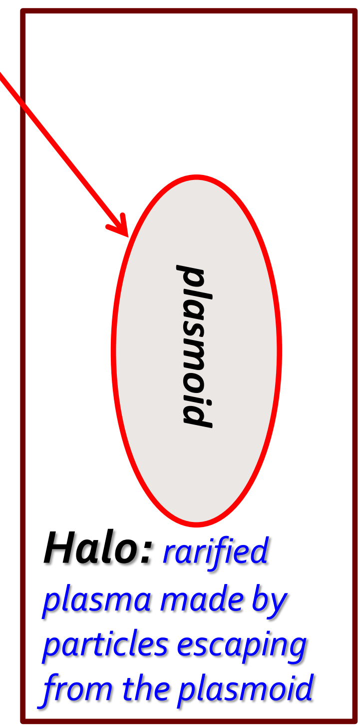

20th topical conference on RF power in plasmas
Sorrento (Italy), June 24-28, 2013

Self-consistency implementation
Full-wave calculation with FEM method

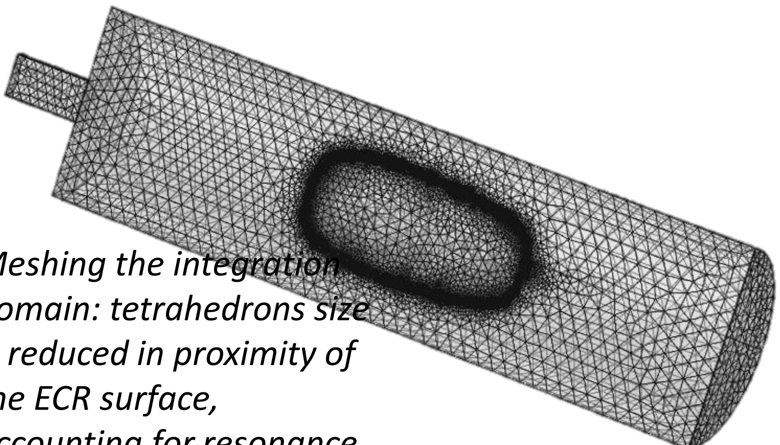

Meshing the integration domain: tetrahedrons size is reduced in proximity of the ECR surface, accounting for resonance.

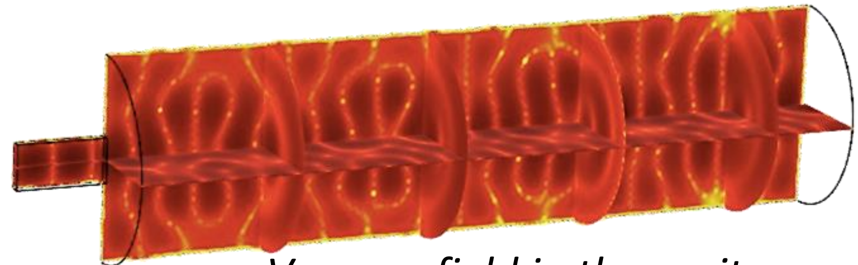

Vacuum field in the cavity

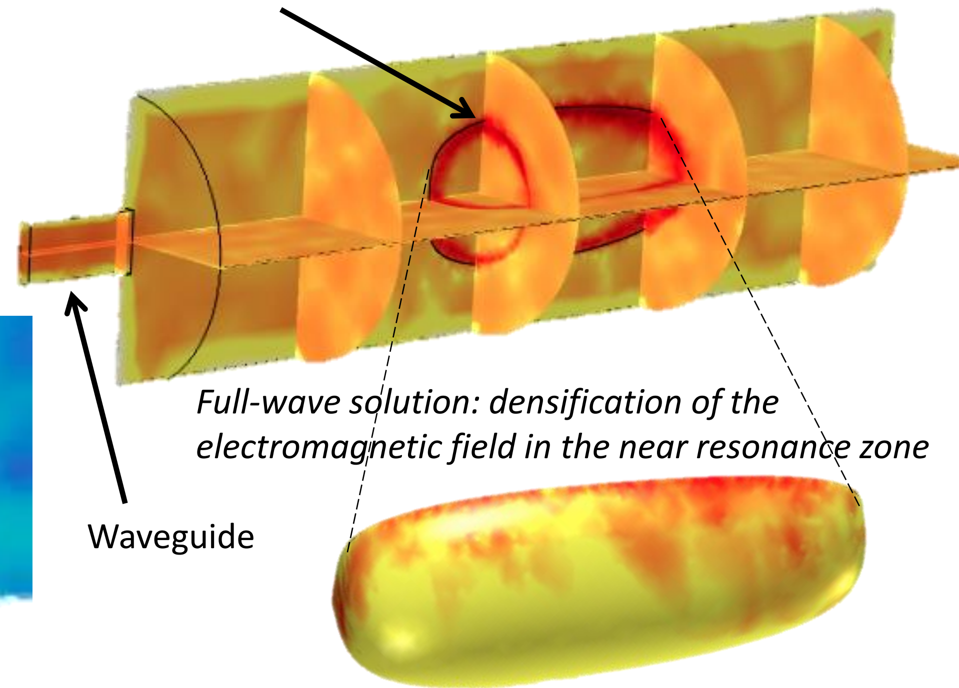

Full-wave solution: densification of the electromagnetic field in the near resonance zone

Areas where the electric field is more intense:
The plot is in log colour map

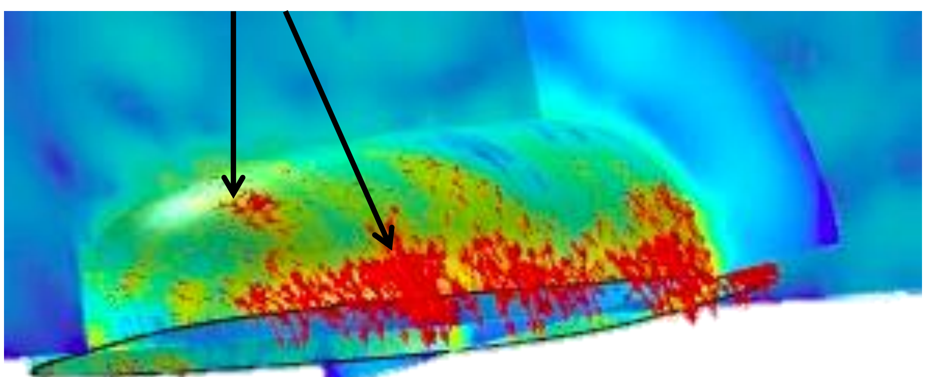

Plasma Diagnostics

- Advancements in X-ray spectroscopy (including space-resolved spectroscopy)
- Development of a new, compact microwave interferometer

Advanced techniques of plasma diagnostics have been already implemented: the X-ray pin-hole camera

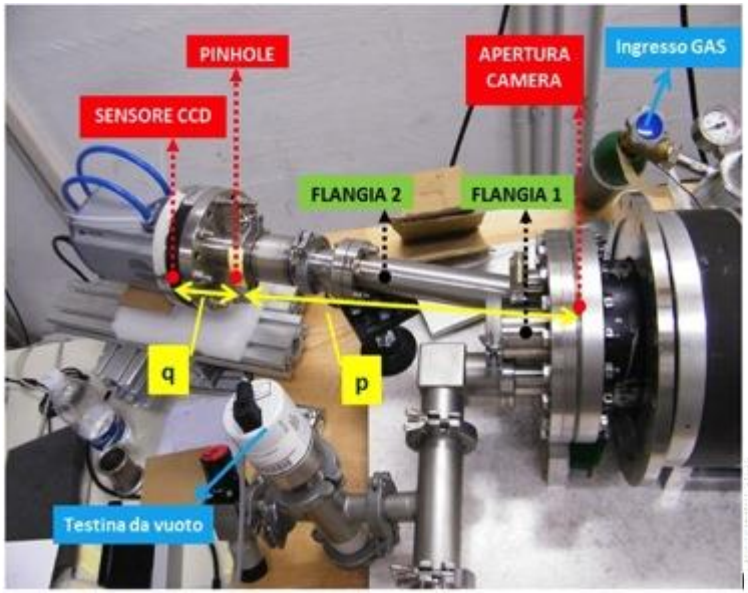

X-ray imaging can be performed with a pin-hole camera technique

The pin-hole is mounted between the plasma and a X-ray sensitive CCD camera having 1024x1024 pixels in the 0.5-15 keV energy domain

X-ray sensitive CCD - camera

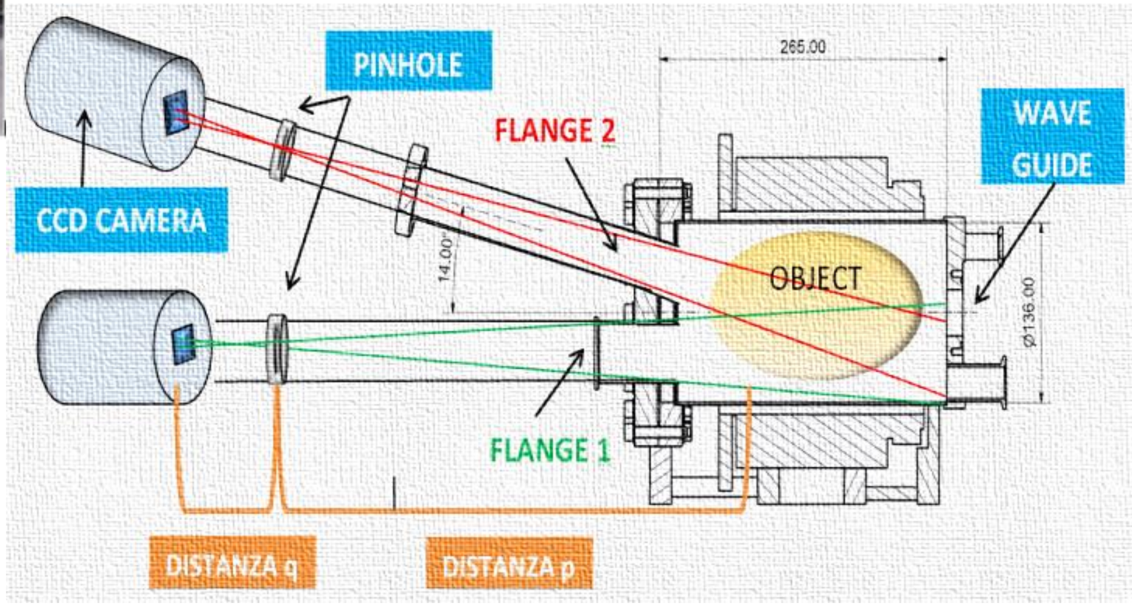

Plasma wave formation is highlighted by X-ray emission: Setup for X-ray spectroscopy

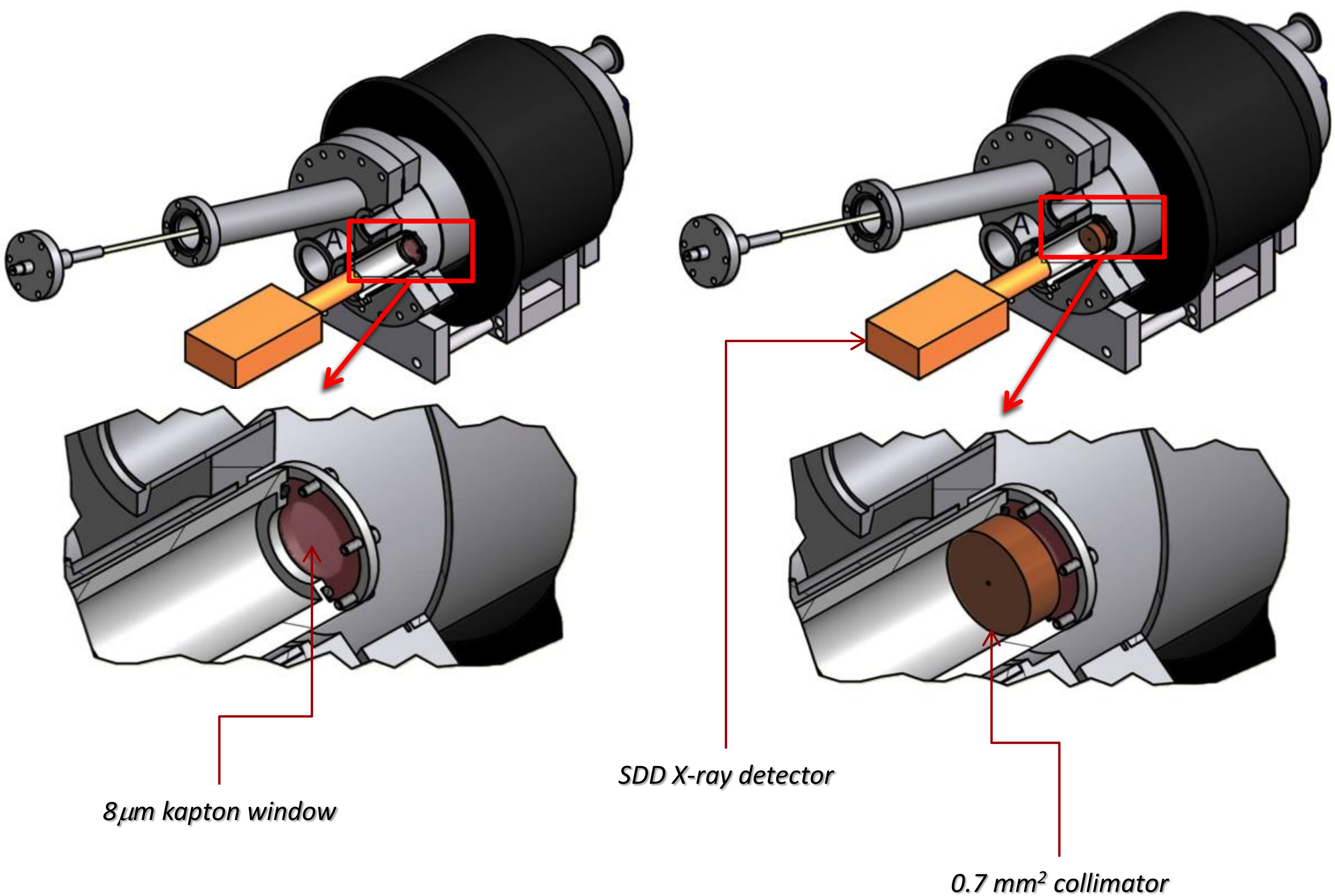

X-ray diagnostics for spectrometry and imaging

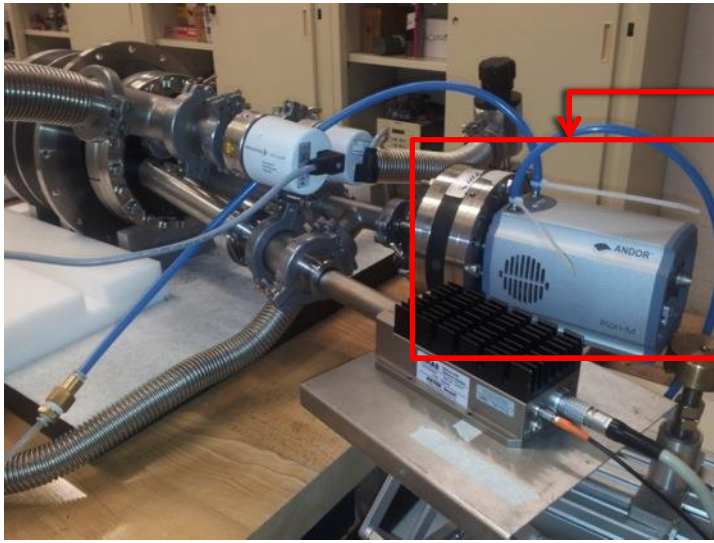

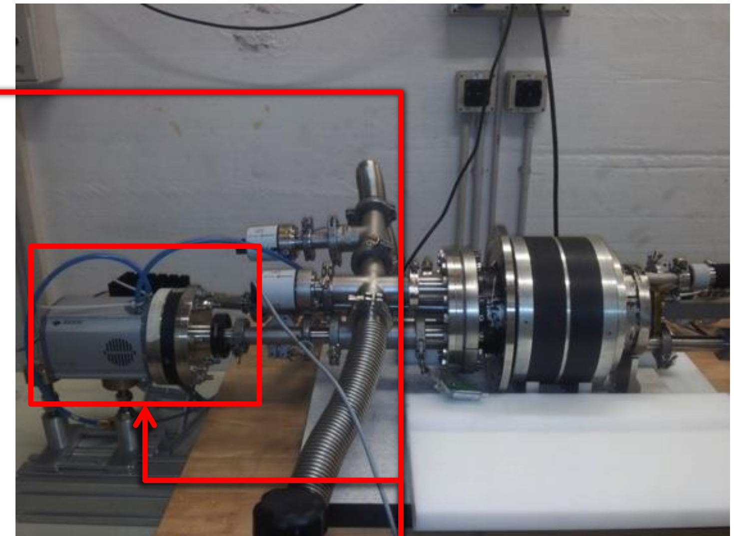

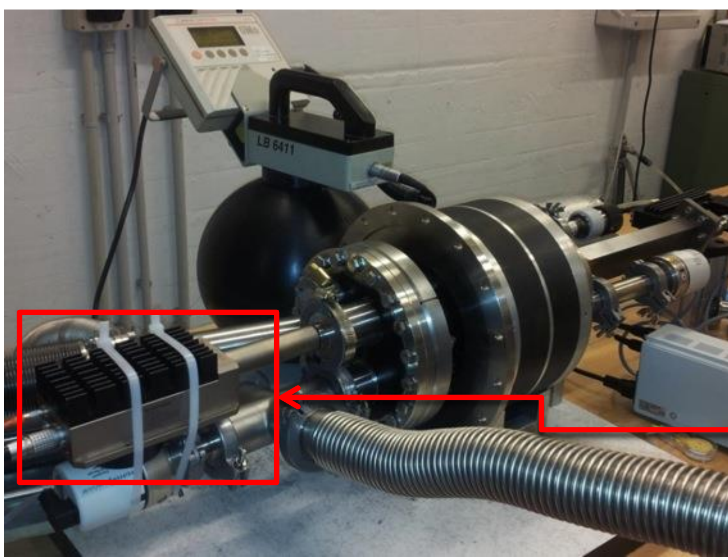

CDD-Camera by ANDOR

IKON-M 934 DO series
Sensor size 13.3x13.3 mm
1024x1024 pixels
Pixel size 13.3 um
Max readout rate 5MHz
Cooling up to -100°C

SDD –detector by KETEK

25 micron Be windows (*very low efficiency @1-2kev*)
80 mm^2 active sirface
160 eV @ 5.9 keV
Operative conditions: up to 500 kcps at 2.1 usec. peaking time

X-ray imaging: detection of the Hot Electron Layer

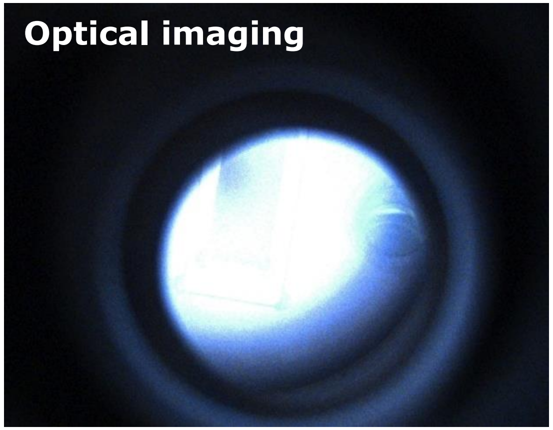

Images in the optical window, taken through an off-axis DN40 flange, evidence the generation of a high-brightness annulus surrounding a dark hole.

X-ray imaging evidences that the pumping power is deposited in the annulus, where the energetic electrons are generated

Transversal reconstruction of the plasma structure in X-ray domain (1-30 keV).

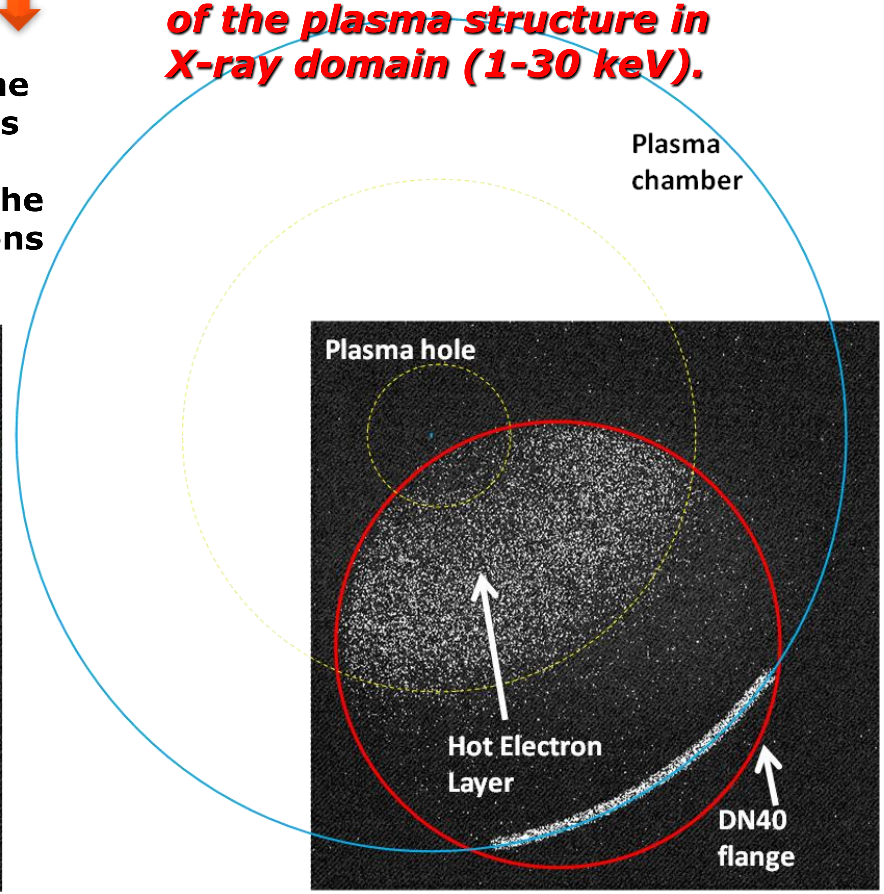

A high brightness strip appears due to electrons impinging on the chamber walls (bremsstrahlung through the stainless steel walls)

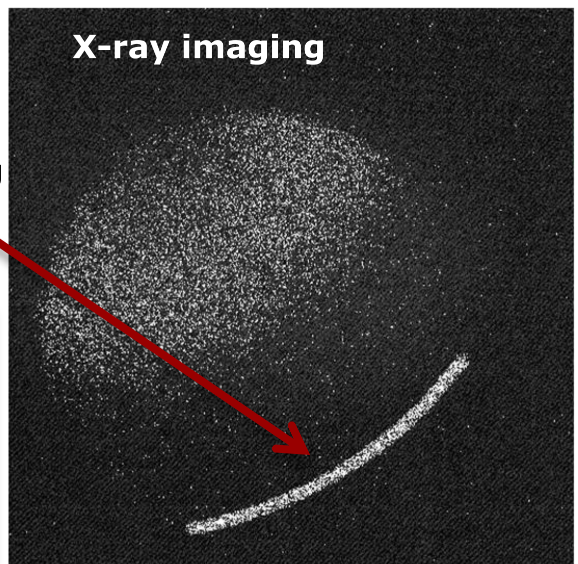

gas:Argon
pressure:3*10-4 mbar
RF power:100W
100 frames - 1sec exposure for each one

Plama Diagnostics: sophisticated tools for covering the entire EM spectrum

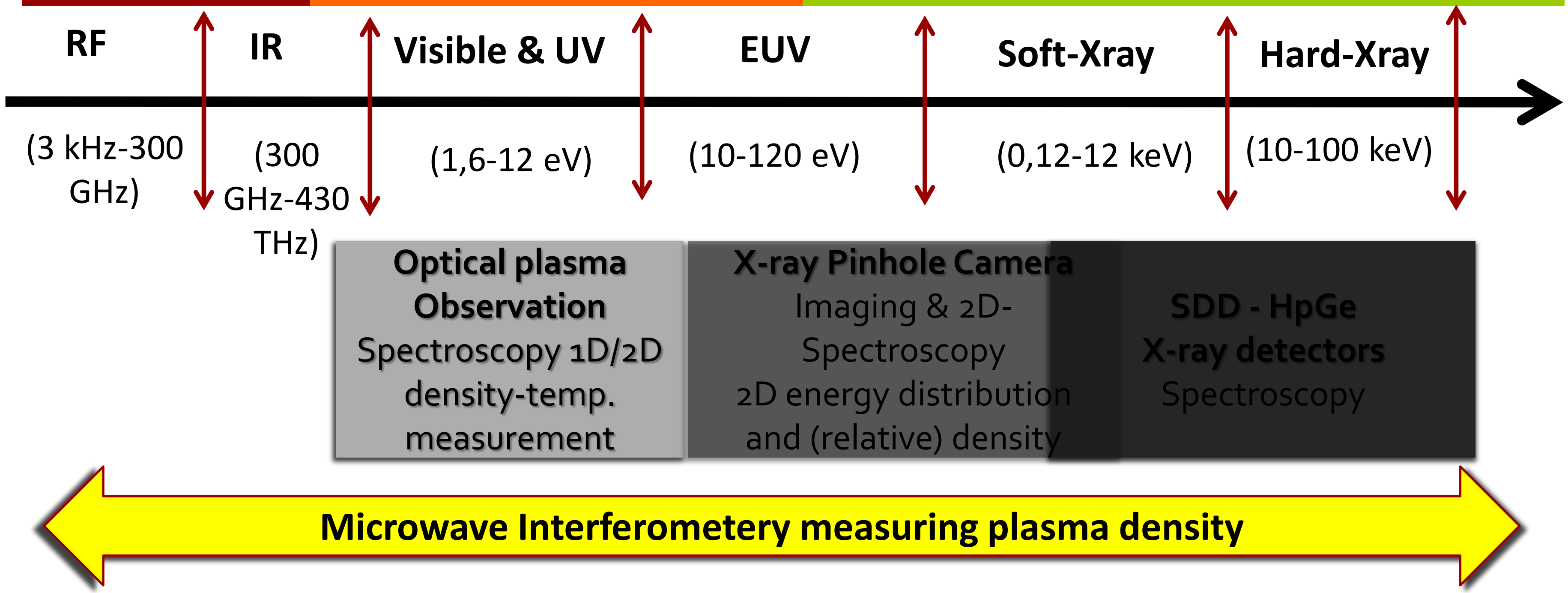

We need a tool able to measure density of electrons with an externally injected "probing" radiation (no perturbation since $P_{probing}/P_{exciting}<1\%$)

→ Density measurement technique no-longer based on plasma emission but on "response-on-transmission" of microwaves through the plasma

MICROWAVE INTERFEROMETRY

Interferometry for plasmas

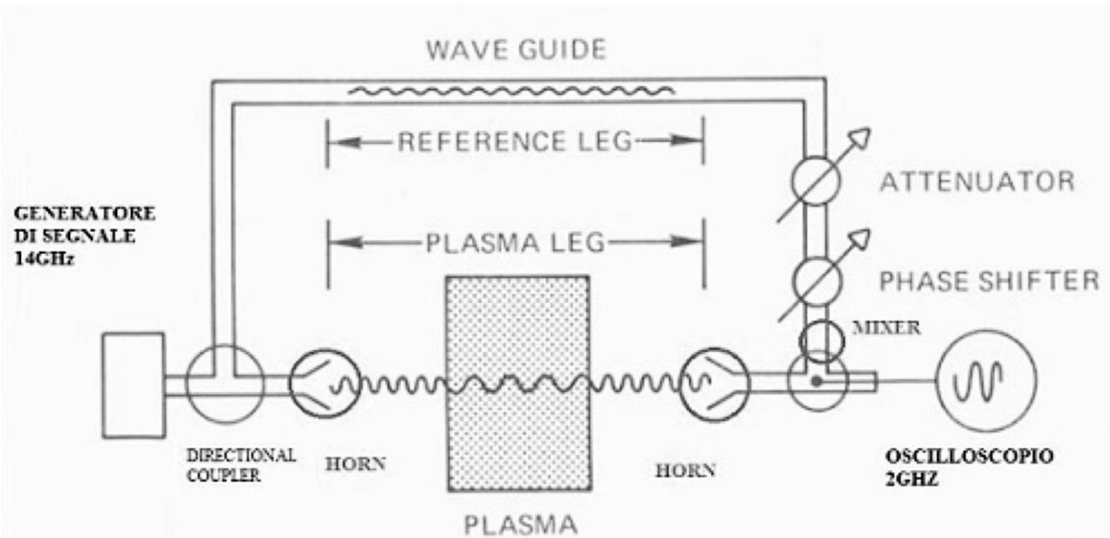

Classical Scheme of Interferometer

$$\Delta\varphi = \frac{\omega}{c}\left[1 - \left(1 - \frac{{\omega_p}^2}{\omega^2}\right)^{\frac{1}{2}}\right] L \quad \rightarrow \quad {\omega_p}^2 = \frac{4\pi n e^2}{m\varepsilon_0}$$

In plasmas the phase variation depends on the " natural plasma frequency"

The plasma frequency depends on the density

Microwave interferometry measures plasma density through a measurement of phase shift.

Interferometry for plasmas

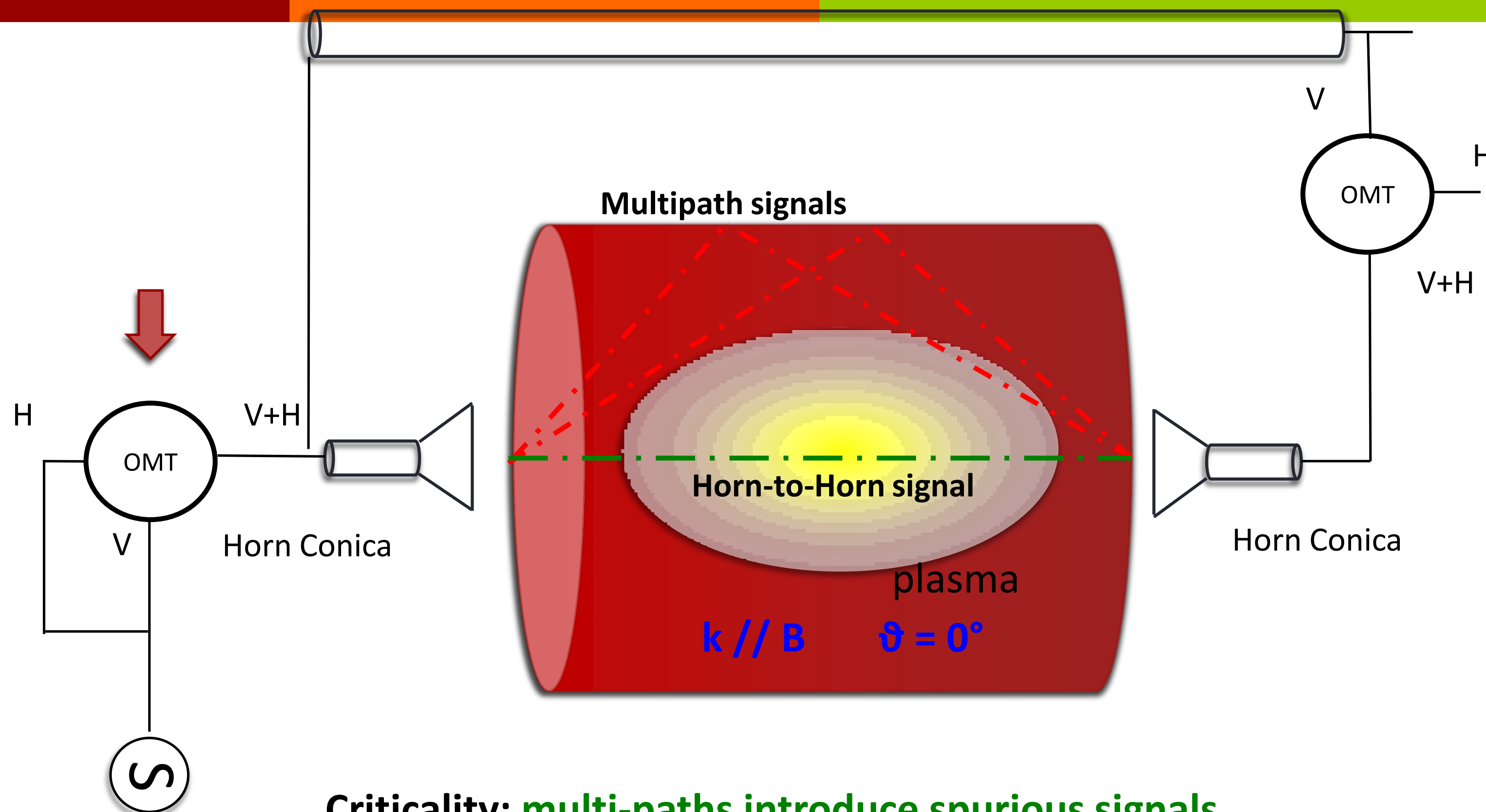

Criticality: multi-paths introduce spurious signals

SIMULATION HORN TO HORN TO UNDERSTAND HOW TO DISCRIMINATE CAVITY WALL EFFECTS IN PROGRESS

Measurements at GSI (March 2013):

impact of the pumping wave frequency on the X-ray spectra for either intermediate and high energy levels

SDD detector *for warm electron component*

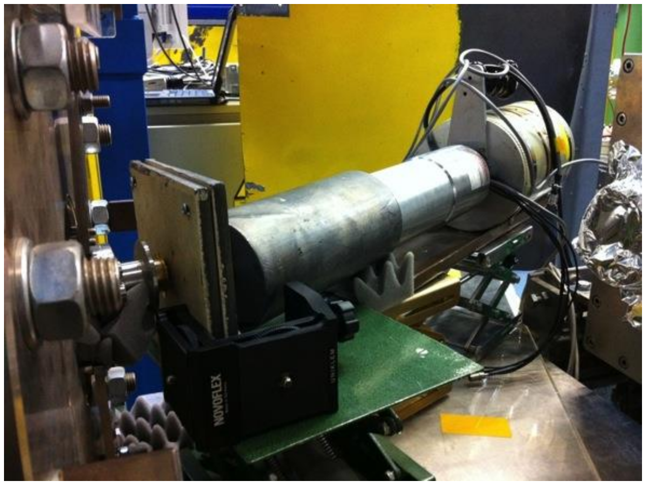

HpGe detector *for hot electron component*

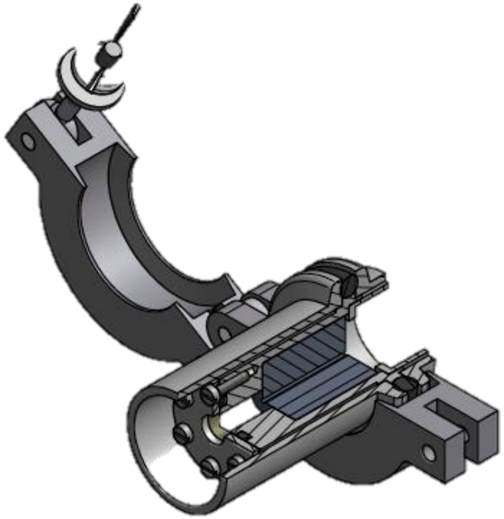

Collimation system *for the detection of the plasma-core (only) X-radiation.*

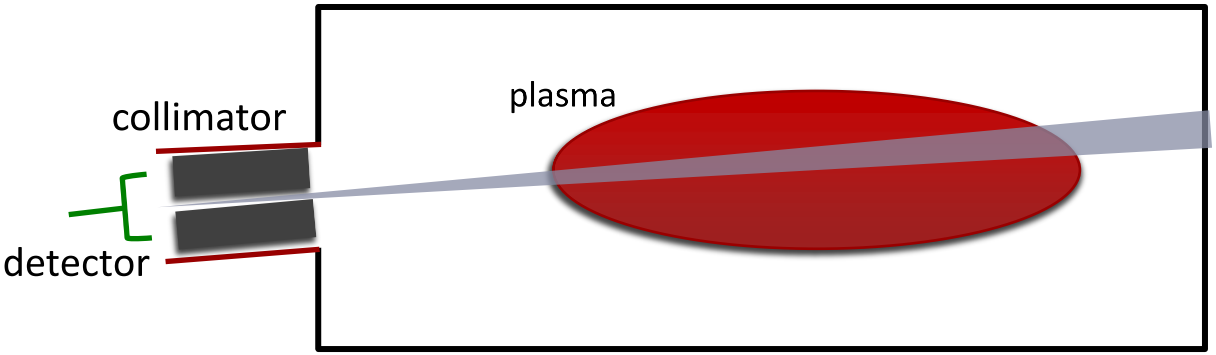

Measuring plasma radiation emission (X-ray domain) in near axis region.

Measurements at GSI:

***impact of the pumping wave frequency on the X-ray spectra for either intermediate and high energy levels* (ARGON PLASMA)**

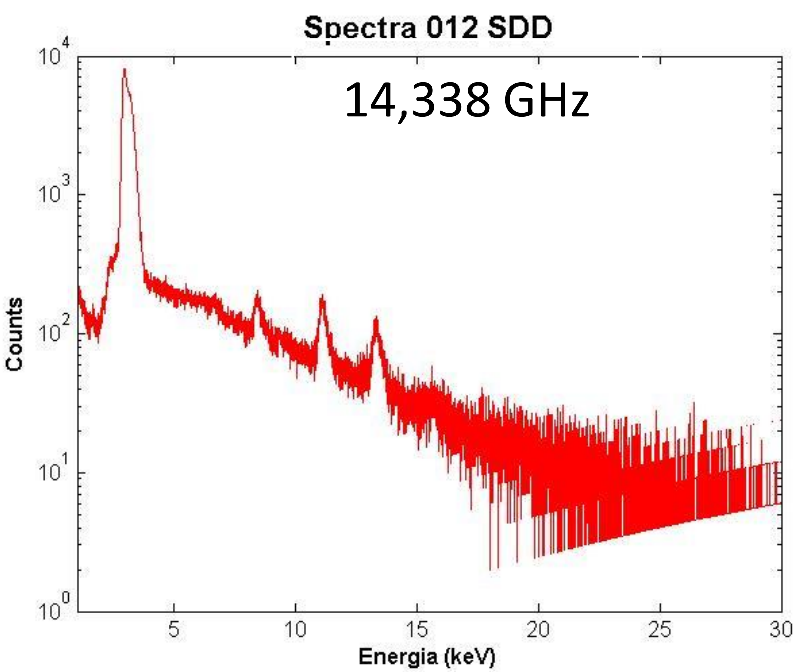

6,5617 keV ± 0,56833622

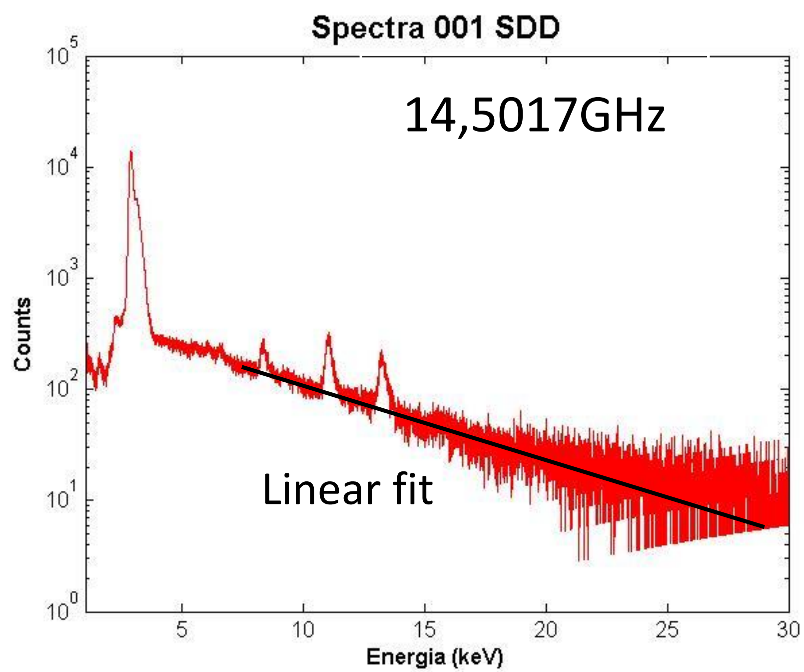

8,5279 keV ± 0,341697613

The fine tuning of the frequency produced strong changes in the energy spectrum, reflecting on the warm plasma temperature.

Measurements at GSI:

impact of the pumping wave frequency on the X-ray spectra for either intermediate and high energy levels

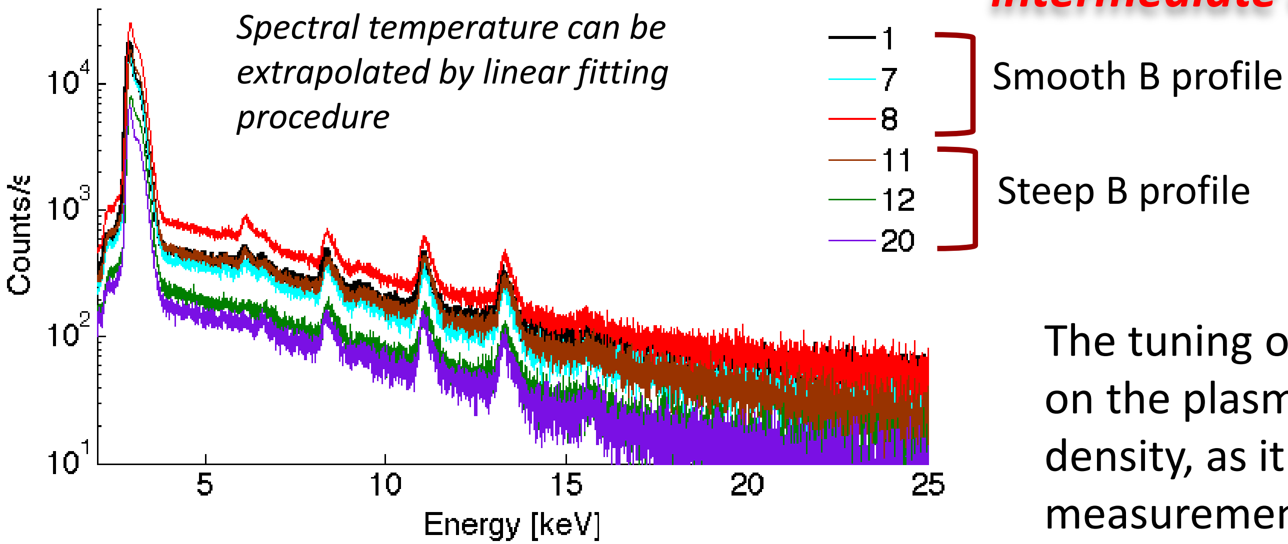

The tuning of the frequency reflects on the plasma temperature and density, as it comes ort from X-ray measurements

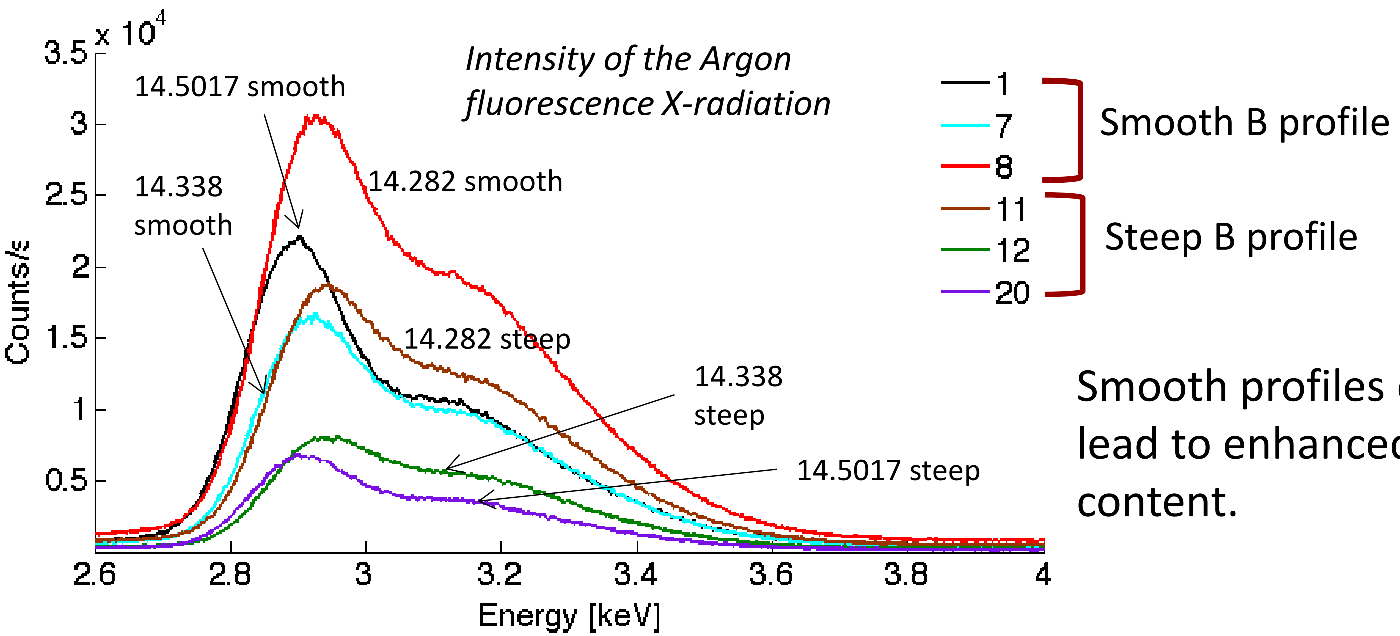

Smooth profiles of the magnetic field lead to enhanced plasma energy content.

Measurements at GSI:

Warm

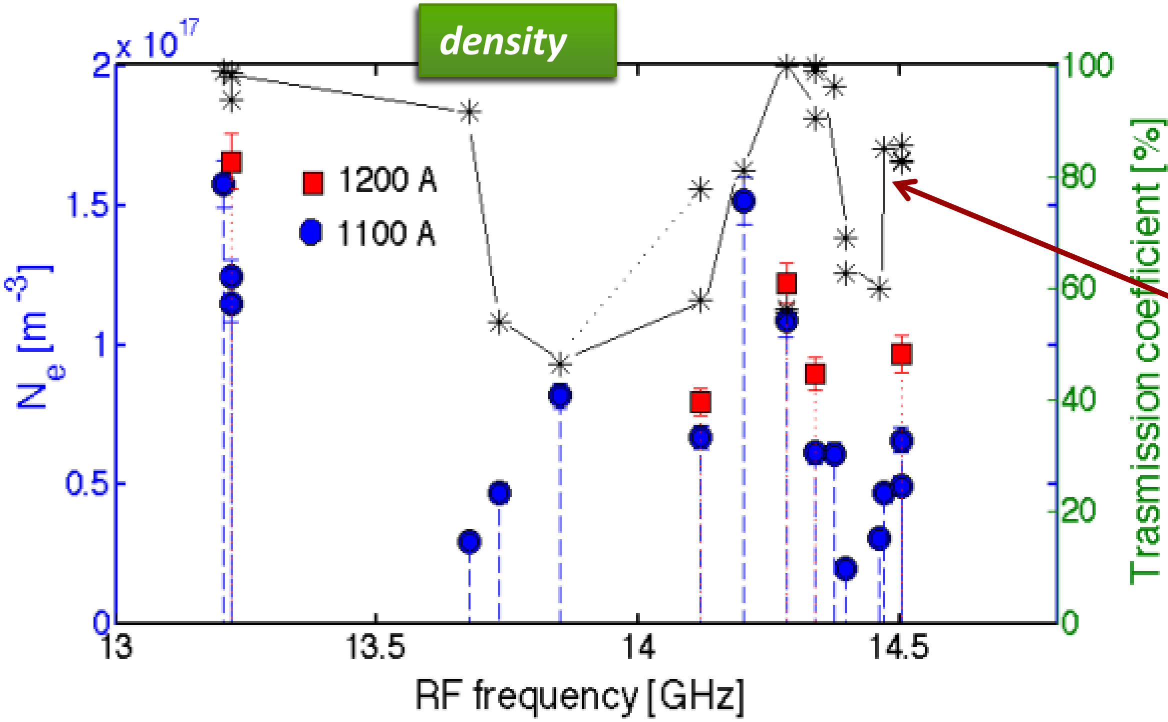

Density fluctuations (one order of magnit.!) are often uncorrelated with transmission coefficients. ***No MW coupling issues but Wave-to-Plasma interaction***

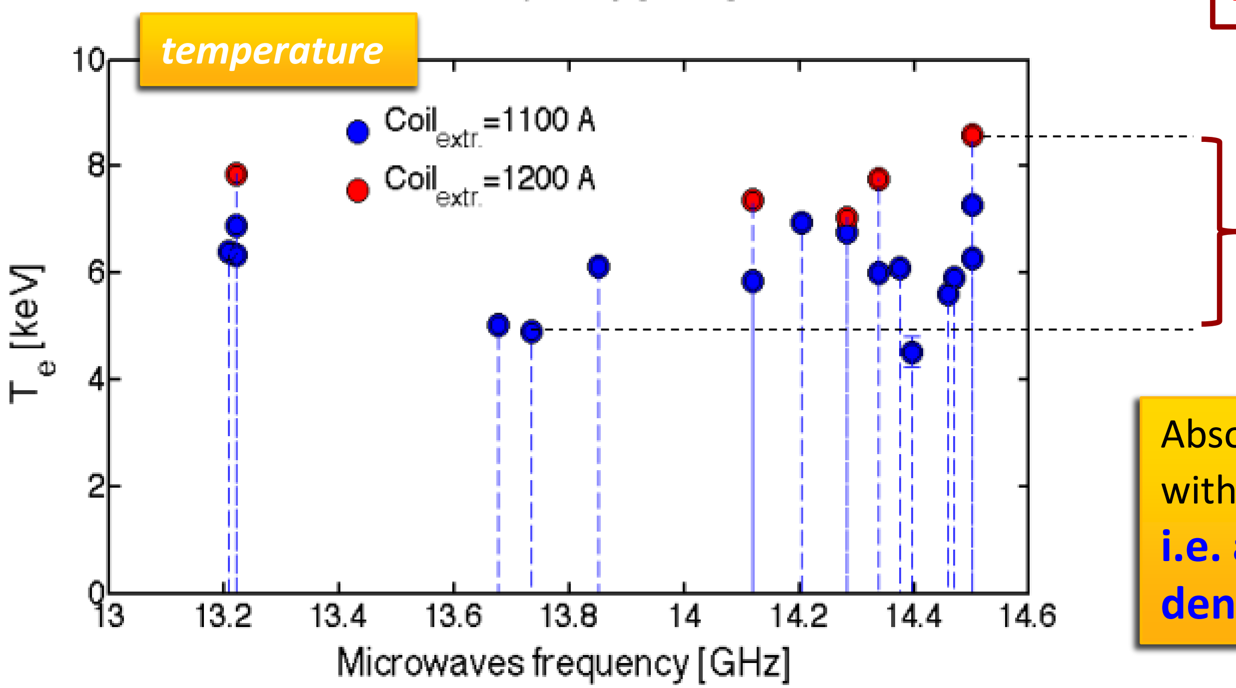

Warm electrons temperature varies in the range 4.2-8 keV

Absolute values of the density are within the range **$0.2\text{-}2\cdot10^{11}$ cm^{-3}, i.e. around 1-10% of the cutoff density at 14 GHz**.

Measurements at ATOMKI :

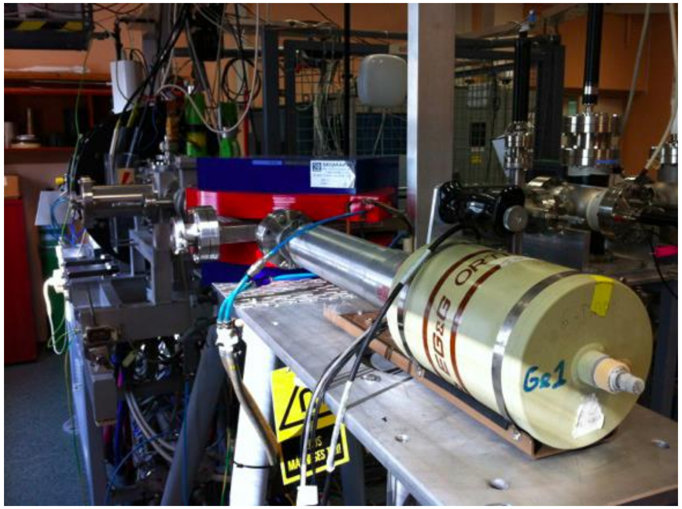

Germanium detector (>30 keV)

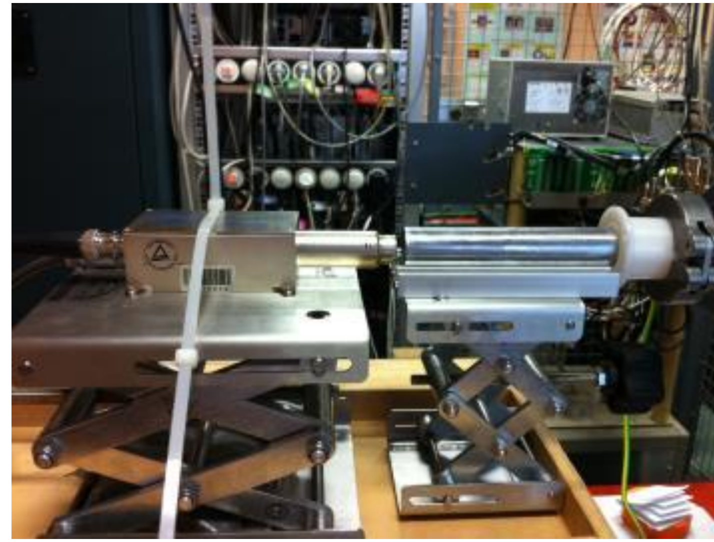

Silicon Drift Detector (2<E<30keV)

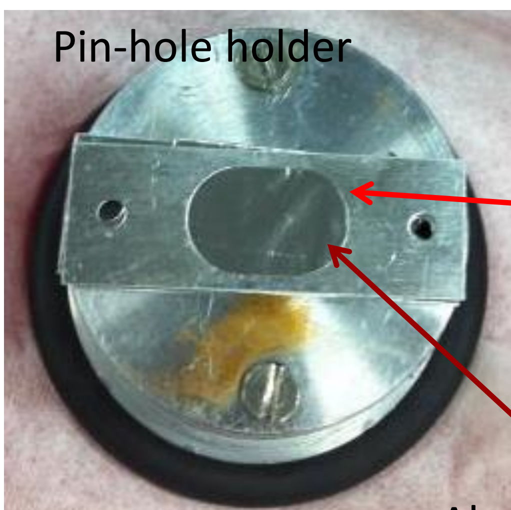

CCD based pin-hole camera (0.5<E<10keV)

Aluminum Window

Measurements at ATOMKI :

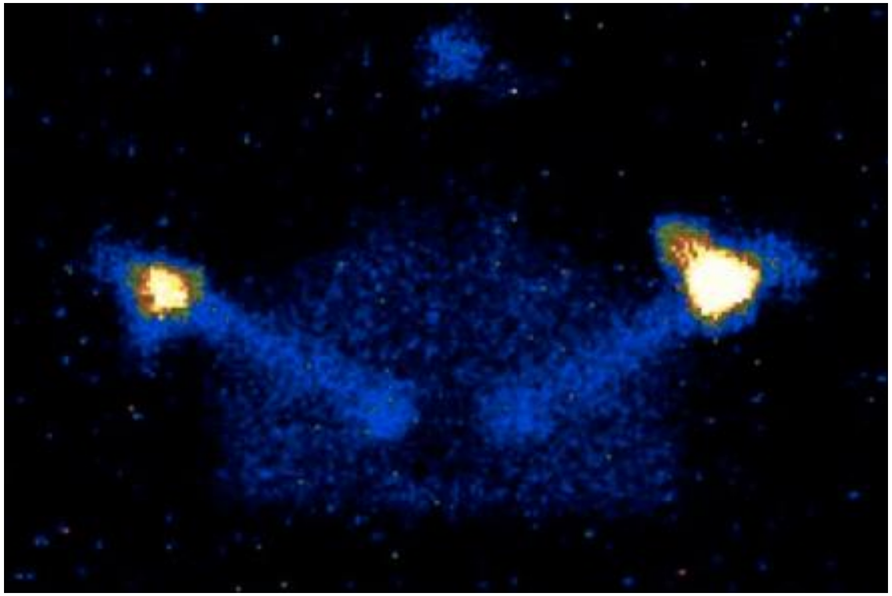

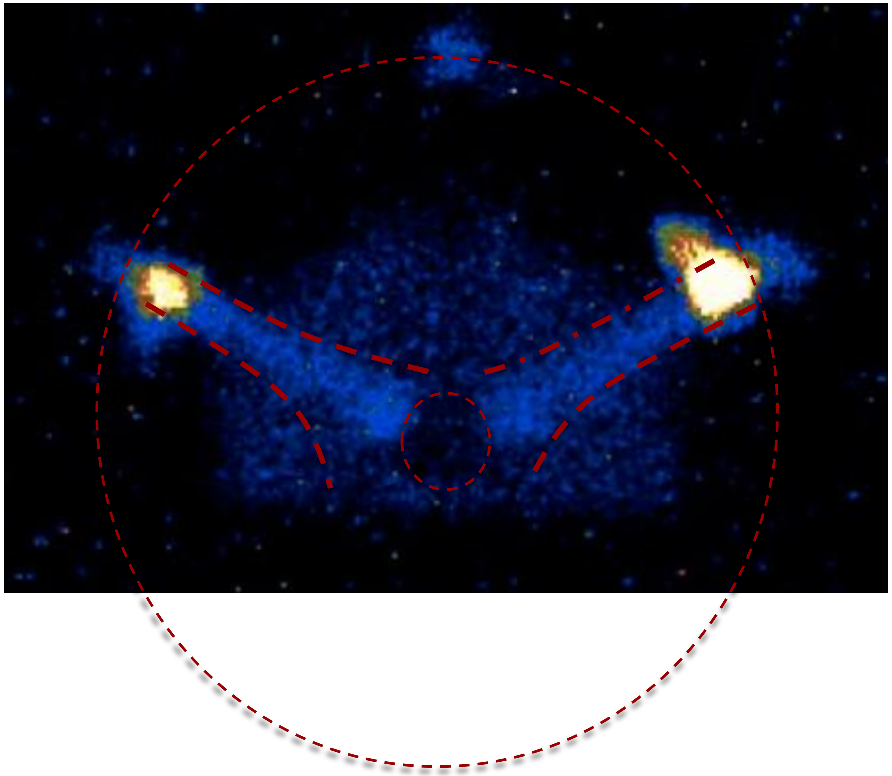

Preliminary results coming out from a 30 W argon plasma, excited at 3.5E-6 mbar, B_{inj}=1.2/B_{min}=0.33/B_{ext}=0.9/B_{hex}=0.9 T.

Just imaging (not yet SRS – Space Resolved Spectroscopy) after 1 second time exposure by 256x1024 (pixels of 26.6x26.6 μm^2) CCD camera in pin-hole mode.

Calcium beams

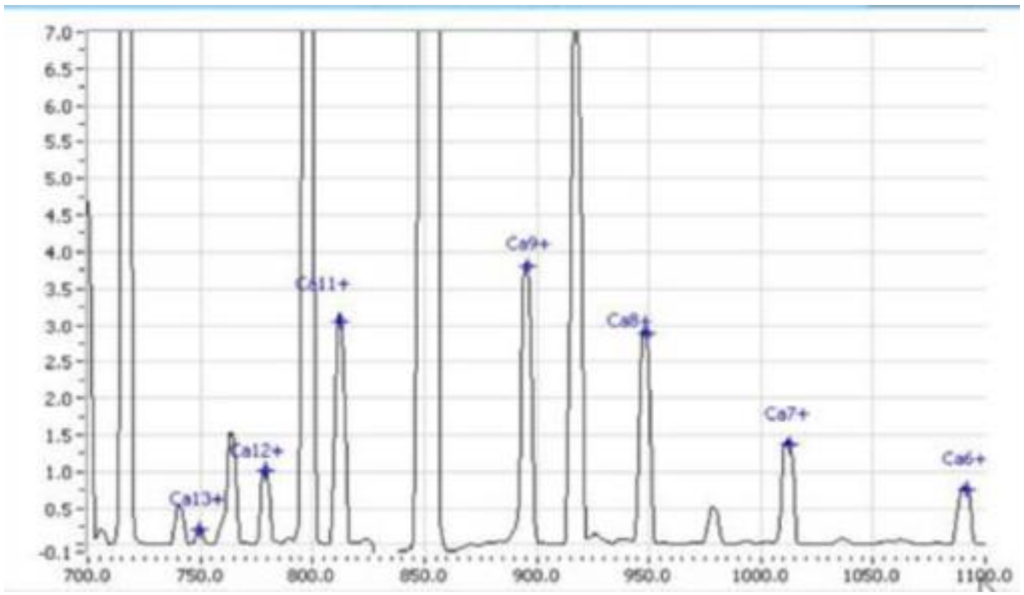

Goal: **Ca^{11+} > 200pnA (source)**

Consumption:

0.23mg/h without the liner (already lower w.r.t. Tandem)

0.16mg/h with liner

Previous configuration:

150pnA can be extracted from the sputtering source for 8 days (max), giving a consumption rate of 0.45 mg/h. This particle current is further reduced after the stripping process inside the Tandem and the overall transmission, leading to a final current of no more than 2.7 pnA after acceleration

Pb an Lithium beams

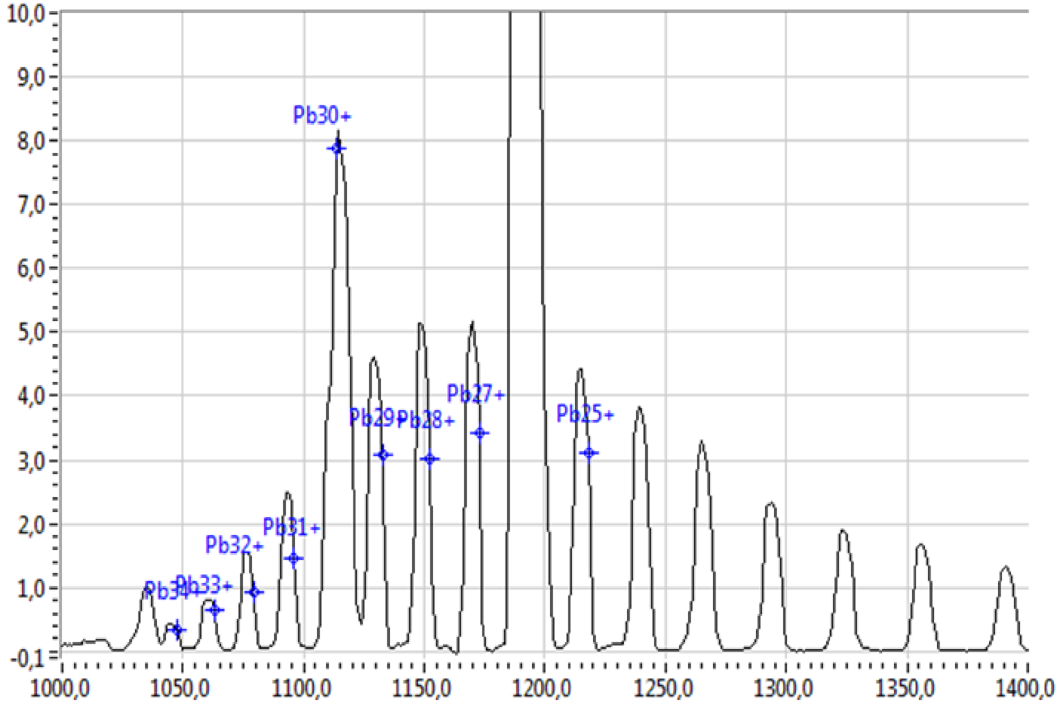

Performance declared by PK:
1 μA of Pb^{27}

Performance achieved:
1.5 μA of Pb^{32+}, leading to a more suitable A/q value of 6.5 with frequency tuning optimization (14.384 GHz)

Lithium: Test will be carried out soon with TFH. Microwaves produced by two TWTs will be mixed together with a 4 port diplexer Hybrid coupler.

AISHa
Advanced Ion Source for Hadrontherapy

Perspectives

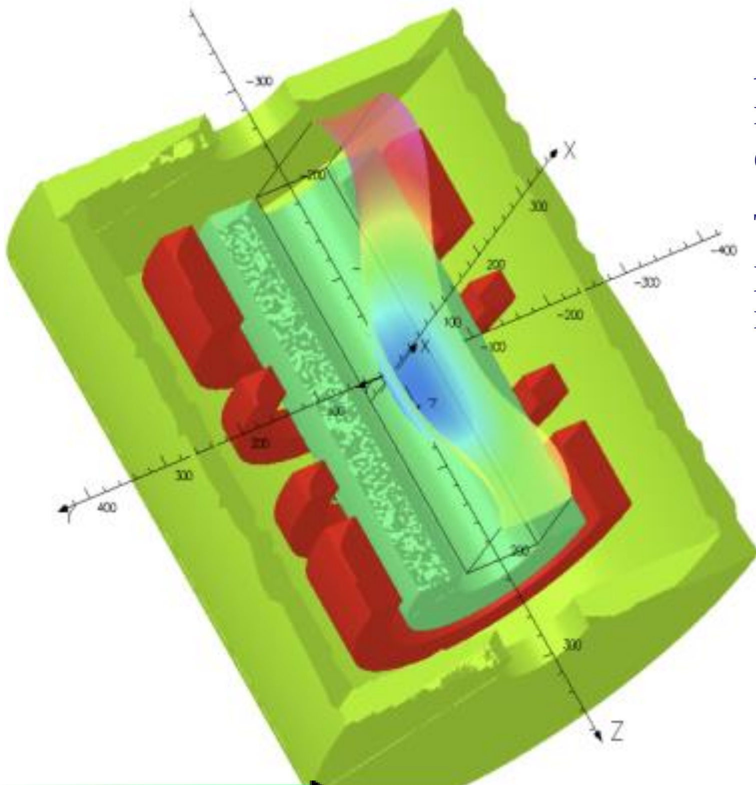

AISHA is a hybrid ECRIS: the radial confining field is obtained by means of a permanent magnet hexapole, while the axial field is obtained with a **Helium-free superconducting system.**

The **operating frequency of 18 GHz will permit** to maximize the plasma density by employing commercial microwave tubes meeting the **needs of the installation in hospital** environments.

Radial field	1.3 T
Axial field	2.7 T - 0.4 T - 1.6 T
Operating frequencies	18 GHz (TFH)
Max operating power	1.5 kW + 1.5 kW
Extraction voltage	40 kV
Chamber diameter / length	Ø 92 mm / 360 mm
LHe	Free
Warm bore diameter	274 mm

AISHa room

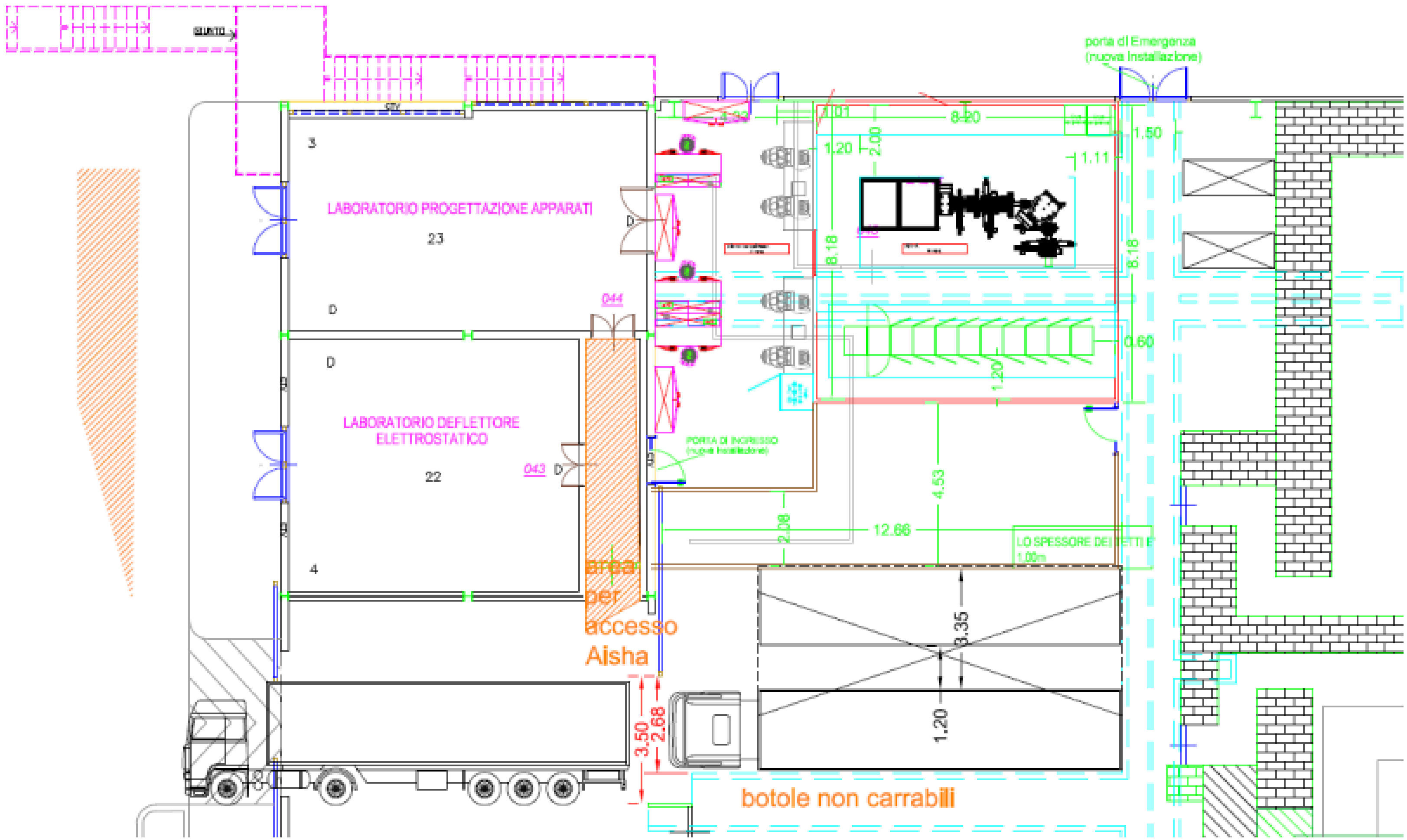
porta di Emergenza
(nuova installazione)
8.20
1.20
2.00
1.50
1.11
LABORATORIO PROGETTAZIONE APPARATI
23
3
D
8.18
8.18
0.60
1.20
044
D
LABORATORIO DEFLETTORE
ELETTROSTATICO
22
043
PORTA DI INGRESSO
(nuova installazione)
4.53
2.08
12.66
LO SPESSORE DEI TETTI E
1.00m
4
area
per
accesso
Aisha
3.35
1.20
3.50
2.68
botole non carrabili

Conclusions

- Modelling implemented, now towards self-consistent calculations
- Development of plasma diagnostic tools (X-ray spatially resolved spectroscopy, microwave interferometer)
- Much more results than expected have come from modelling and stimulated production of plasma waves. Synergy between calculations and measurements.
- Development of metallic beams
- Construction of AISHa (together with ESS and FPT).